Model-Agnostic Linear Estimation of Generator Rotor Speeds based on Phasor Measurement Units

Federico Milano, *Fellow, IEEE*, Álvaro Ortega, *Member, IEEE*, Antonio J. Conejo, *Fellow, IEEE*

***Abstract*— The paper focuses on the estimation of the rotor speeds of synchronous machines by means of phasor measurement units. This estimation is aimed at on-line monitoring of electro-mechanical transients and transient stability analysis. The proposed technique is based on the concept of *frequency divider formula* recently published by the first two authors in these Transactions. The dynamic state estimation is formally stated as a convex optimization problem and a thorough discussion of the sensitivity analysis of the optimal solution is provided. The case study considers a dynamic 1,479-bus model of the all-island Irish system and discusses the effect of bad data, noise and latency on the proposed estimation technique.**

***Index Terms*— Dynamic state estimation (DSE), optimization, phasor measurement unit (PMU), sensitivity analysis, synchronous machine, transient stability analysis.**

I. Introduction

A. Motivations

Dynamic State Estimation (DSE) is a fundamental tool of energy management systems and control centers of transmission system operators. DSE can also be useful for short-term transient stability predictions and has become even more important and challenging with the recent development of the smart grid. This, in fact, typically requires faster and system-wider controls than traditional power systems. With the introduction of Phasor Measurement Units (PMUs), which have a high sampling rate – up to 120 measurements per second – and accurate synchronization, a fast and accurate DSE is now possible. In this vein, the paper proposes an application of PMUs for the on-line estimation of the rotor speeds of synchronous machines.

B. Literature Review

There is a vast literature on DSE. Traditional methods are based on a set of nonlinear Differential-Algebraic Equations (DAEs) that models the machines and the controllers of the system [1]. The nonlinearity of the model is a major challenge, as the solution of the state estimation problem is iterative and requires the calculation and factorization of the Jacobian matrix of the DAEs [2]. Another important aspect of state estimation and, hence, also of DSE, is how to process bad data. With this aim, several techniques mostly based on the Kalman filter have been proposed [3], [4]. Other filtering techniques include, for example, particle filter [5] and mean squared estimator [6]. Finally, decentralization of the state estimation is also important, especially for large systems [7].

With the advent of PMU technology, the state estimation has gained the ability to acquire the measurements of bus voltage and current phase angles. This has led to a variety of new state-estimation models, mostly coupled with the Extended Kalman Filter (EKF) [8]–[11]. In [12], frequency measurements from PMUs are also utilized.

The models discussed so far are based on nonlinear DAEs. References [13] and [14] propose linear state estimation models. In all these works, the models of the synchronous machines and their controllers as well as of dynamic loads has to be defined *a priori*. The same requirement affects the approaches discussed in [15]–[17], which are aimed at estimating the states of the machines using local PMUs measurements.

The approach proposed in this paper is conceptually different from the current state of the art. We propose, in fact, a linear and model-independent rotor-speed estimation problem based on the concept of the Frequency Divider Formula (FDF) [18]–[20]. *Model-independent* means that generator and load dynamic models and parameters need not to be known. The FDF only requires the bus frequencies measured by PMUs, not voltage and current phasors. The proposed technique is a novel application of the FDF, which, in recent works, has been utilized to estimate bus frequencies [21], and the frequency of the Center of Inertia (COI) [22].

In [18], the FDF was utilized in simulations to capture local bus frequencies based on the exact values of the machine rotor speeds. In a simulation tool, the vector of rotor speeds is accessible at any time and thus the FDF is a consistent and reliable tool. Transmission system operators, however, can install PMUs at network buses, and have thus access to the bus frequencies estimated by such PMUs, while the rotor speeds of the synchronous machines are not accessible to them. This paper considers a practical application of the FDF based on available real-world measurements.

C. Contributions

Specific contributions of the paper are the following:

- A linear, model-agnostic optimization problem that estimates the rotor speeds of synchronous machines based on the FDF and PMU frequency measurements.
- A comparison of the proposed optimization problem and a conventional Weighted Least Square (WLS) approach.

Federico Milano and Álvaro Ortega are with the School of Electrical and Electronic Engineering, University College Dublin, Belfield, Ireland. E-mails: alvaro.ortegamanjavacas@ucd.ie; federico.milano@ucd.ie

Antonio J. Conejo is with Department of Integrated Systems Engineering and the Department of Electrical and Computer Engineering, The Ohio State University, Columbus, OH 43210, USA. E-mail: conejonavarro.1@osu.edu

This material is based upon works supported by the European Commission Ireland, by funding Á. Ortega and F. Milano, under the RESERVE Consortium, Grant No. 727481. F. Milano is also funded by the Science Foundation Ireland, under Investigator Programme, Grant No. SFI/15/IA/3074.

- An analytical expression that defines the minimum set of PMU measurements required to estimate rotor speeds.
- A discussion on the tradeoff between centralized and decentralized versions of the proposed DSE.
- A sensitivity analysis of the impact of bad data, noise and latency on the solution of the proposed DSE.

The sensitivity analysis is inspired on the seminal works on mathematical programming [23]–[25], which have been applied to the analysis of power system operation [26], [27] as well as to the classical state estimation problem [28].

D. Paper Organization

The remainder of the paper is organized as follows. Section II outlines the formulation of the FDF while Section III describes the formulation of the proposed rotor-speed estimation problem and the sensitivity analysis of the optimal solution. The formulation of the standard WLS problem is also given in Section III. Section IV illustrates the properties of the proposed technique by means of the WSCC 9-bus, 3-machine test system. The case study is provided in Section V and is based on a 1,479-bus dynamic model of the all-island Irish transmission network and considers different scenarios with bad data, noise and latency. Finally, Section VI duly draws conclusions and outlines future work directions.

II. Frequency Divider Formula

In [18], the first two authors have proposed an analytical approach to calculate the bus frequencies based on the FDF. The mathematical background of the FDF is the augmented admittance matrix of the system and the assumption that the frequency along the impedances of transmission lines varies as in a *continuum matter* where synchronous machine rotor speeds define boundary conditions. A detailed discussion on the assumptions and hypotheses behind the definition of the FDF are beyond the scope of this paper. Full details are provided in [18], to which we refer the interested reader. In the remainder of this section, we briefly outline the expression and relevant properties of the FDF.

Let consider a network with n buses and m synchronous machines. The starting point is the augmented admittance matrix, which is discussed in many books, e.g., [29]. Apart from the transmission system connections, this matrix also includes the m nodes of the electromotive forces behind the internal reactances of the synchronous machines. The resulting matrix has the following shape:

$$\bar{\mathbf{Y}} = \begin{bmatrix} \bar{\mathbf{Y}}_{\text{GG}} & \bar{\mathbf{Y}}_{\text{GB}} \\ \bar{\mathbf{Y}}_{\text{BG}} & \bar{\mathbf{Y}}_{\text{BB}} \end{bmatrix} , \tag{1}$$

where the subscripts G and B stand for generator buses, and for load and transition buses, respectively, and $\bar{\mathbf{Y}}_{\text{GG}} \in \mathbb{C}^{m\times m}$, $\bar{\mathbf{Y}}_{\text{BB}} \in \mathbb{C}^{n\times n}$; $\bar{\mathbf{Y}}_{\text{GB}} \in \mathbb{C}^{m\times n}$; and $\bar{\mathbf{Y}}_{\text{BG}} \in \mathbb{C}^{n\times m}$. The submatrix $\bar{\mathbf{Y}}_{\text{BB}}$ is:

$$\bar{\mathbf{Y}}_{\text{BB}} = \bar{\mathbf{Y}}_{\text{bus}} + \bar{\mathbf{Y}}_{\text{G}} , \tag{2}$$

where $\bar{\mathbf{Y}}_{\text{bus}}$ is the well-known network admittance matrix, and $\bar{\mathbf{Y}}_{\text{G}}$ is a diagonal matrix whose i-th diagonal element is 0 if no machine is connected to bus i, and the inverse of a machine internal transient reactance if such a machine is connected at bus i. As discussed in [30], $\bar{\mathbf{Y}}_{\text{BB}}$ is full rank.

Based on (1), the FDF is defined as:

$$\mathbf{0}_{n,1} = \mathbf{B}_{\text{BB}}(\boldsymbol{\omega}_{\text{B}} - \omega_0\mathbf{1}_{n,1}) + \mathbf{B}_{\text{BG}}(\boldsymbol{\omega}_{\text{G}} - \omega_0\mathbf{1}_{m,1}) , \tag{3}$$

where $\boldsymbol{\omega}_{\text{G}} \in \mathbb{R}^m$, is the vector of machine rotor speeds; $\boldsymbol{\omega}_{\text{B}} \in \mathbb{R}^n$, are the frequencies at the system buses; ω_0 is the nominal system frequency; and

$$\mathbf{B}_{\text{BB}} = \text{Im}\{\bar{\mathbf{Y}}_{\text{BB}}\} , \qquad \mathbf{B}_{\text{BG}} = \text{Im}\{\bar{\mathbf{Y}}_{\text{BG}}\} ,$$

where $\mathbf{B}_{\text{BB}}$ has same rank and symmetry properties as $\bar{\mathbf{Y}}_{\text{BB}}$.

To simplify the notation, we rewrite (3) in terms of frequency deviations with respect to the nominal frequency ω_0, as follows:

$$\mathbf{0}_{n,1} = \mathbf{B}_{\text{BB}}\Delta\boldsymbol{\omega}_{\text{B}} + \mathbf{B}_{\text{BG}}\Delta\boldsymbol{\omega}_{\text{G}} , \tag{4}$$

where $\Delta\boldsymbol{\omega}_{\text{B}} = \boldsymbol{\omega}_{\text{B}} - \omega_0\mathbf{1}_{n,1}$ and $\Delta\boldsymbol{\omega}_{\text{G}} = \boldsymbol{\omega}_{\text{G}} - \omega_0\mathbf{1}_{m,1}$. In [18], bus frequency deviations are expressed explicitly as

$$\Delta\boldsymbol{\omega}_{\text{B}} = -\mathbf{B}_{\text{BB}}^{-1}\mathbf{B}_{\text{BG}}\Delta\boldsymbol{\omega}_{\text{G}} = \mathbf{D}\Delta\boldsymbol{\omega}_{\text{G}} . \tag{5}$$

In the DSE optimization problem presented in the next section, we utilize the *acasual* expression (4) as matrices $\mathbf{B}_{\text{BB}}$ and $\mathbf{B}_{\text{BG}}$ are very sparse whereas matrix $\mathbf{D} = -\mathbf{B}_{\text{BB}}^{-1}\mathbf{B}_{\text{BG}}$ is dense and its calculation can be cumbersome for large systems.

Equation (4) expresses the dependency of bus frequencies on the rotor speeds, which are weighted based on their electrical proximity, not their inertia. However, since the internal admittance of each machine is, in per unit, proportional to the capacity of the machine itself, bigger machines weight more than smaller ones in the system.

The frequency estimation method discussed in the remainder of the paper is intended to be a tool for TSOs, which generally have full knowledge of the transmission network, but might not have the detailed dynamic models and measurements of internal quantities of the power plants and the loads connected to the grid. The assumption, implied in the FDF, of knowing generator internal impedances is acceptable as the values of such impedances can be easily obtained from the literature and manufacturer data sheets once the technology and the capacity of the power plant is known.

III. Rotor-Speed Estimation

This section is organized as follows. The proposed rotor-speed estimation technique based on a convex quadratic programming problem and the FDF is presented in Subsection III-A. Subsection III-B discusses a standard WLS problem that serves to discuss measurement redundancy and define the minimum set of measurements required to estimate rotor speed based on the FDF. Finally, Subsection III-C presents a systematic approach to calculate all sensitivities of the estimation problem given in Subsection III-A.

A. Proposed Optimization Problem

The proposed frequency dynamic state estimation is formulated as the following optimization problem:

$$\min_{(\boldsymbol{e}_{\text{B}},\,\Delta\boldsymbol{\omega}_{\text{G}})} \quad J = \frac{1}{2}\boldsymbol{e}_{\text{B}}^T\mathbf{W}\boldsymbol{e}_{\text{B}} \tag{6}$$

$$\text{s.t.} \quad \mathbf{0} = \mathbf{B}_{\text{BG}}\Delta\boldsymbol{\omega}_{\text{G}} + \mathbf{B}_{\text{BB}}(\Delta\tilde{\boldsymbol{\omega}}_{\text{B}} + \boldsymbol{e}_{\text{B}}) \qquad : \boldsymbol{\mu}_{\text{B}} , \tag{7}$$

where $\Delta\tilde{\omega}_{\rm B}$ is the input vector of measured bus frequency deviations as provided by the PMUs; $\boldsymbol{e}_{\rm B}$ is the vector of measurement errors; $\Delta\boldsymbol{\omega}_{\rm G}$ is the vector of estimated rotor speed deviations of the synchronous machines; $\boldsymbol{\mu}_{\rm B}$ are the dual variables associated with the equality constraints; and the weight matrix $\mathbf{W}$ is defined as $\mathbf{W} = \text{diag}\{w_1, w_2, \ldots, w_{n-1}, w_n\}$, where $w_i = 1/\sigma_i^2$ and σ_i^2 is the variance of the i-th measurement error $e_{{\rm B}i}$. Equation (6) is the conventional objective function that is generally used in state estimation. While other expressions can be utilized, (6) allows properly illustrating the effectiveness of the proposed technique as it resembles the conventional state estimation problem that is commonly solved in practice.

Matrix $\mathbf{B}_{\rm BG}$ is maximum rank, i.e., m, and $\mathbf{B}_{\rm BB}$ is full rank, i.e., n, hence the gradient vectors of the constraints (7) at the solution are linearly independent. The problem (6)-(7) has thus the required regularity conditions. Moreover, since $\mathbf{W}$ is positive definite, problem (6)-(7) is a convex quadratic programming problem, whose solution is unique [31].

The Lagrangian function $\mathcal{L}(\boldsymbol{\omega}_{\rm G}, \boldsymbol{e}_{\rm B}, \boldsymbol{\mu}_{\rm B})$ associated with the optimization problem (6)-(7) is:

$$\mathcal{L} = J(\boldsymbol{e}_{\rm B}) - \boldsymbol{\mu}_{\rm B}^T \cdot \left[\mathbf{B}_{\rm BG}\Delta\boldsymbol{\omega}_{\rm G} + \mathbf{B}_{\rm BB}(\Delta\tilde{\boldsymbol{\omega}}_{\rm B} + \boldsymbol{e}_{\rm B})\right] . \tag{8}$$

Assuming an input vector of measurements $\tilde{\boldsymbol{\omega}}_{\rm B}$ and the optimal solution $(\boldsymbol{\omega}_{\rm G}^*, \boldsymbol{e}_{\rm B}^*, \boldsymbol{\mu}_{\rm B}^*)$ of problem of (6)-(7), the first order optimality conditions are:

$$\mathbf{0}_{m,1} = \left.\frac{\partial\mathcal{L}}{\partial\Delta\boldsymbol{\omega}_{\rm G}}\right|_* = -\mathbf{B}_{\rm BG}^T\boldsymbol{\mu}_{\rm B}^* , \tag{9}$$

$$\mathbf{0}_{n,1} = \left.\frac{\partial\mathcal{L}}{\partial\boldsymbol{e}_{\rm B}}\right|_* = \mathbf{W}\boldsymbol{e}_{\rm B}^* - \mathbf{B}_{\rm BB}^T\boldsymbol{\mu}_{\rm B}^* , \tag{10}$$

$$\mathbf{0}_{n,1} = \left.\frac{\partial\mathcal{L}}{\partial\boldsymbol{\mu}_{\rm B}}\right|_* = -\mathbf{B}_{\rm BG}\Delta\boldsymbol{\omega}_{\rm G}^* - \mathbf{B}_{\rm BB}(\Delta\tilde{\boldsymbol{\omega}}_{\rm B} + \boldsymbol{e}_{\rm B}^*) . \tag{11}$$

As it is thoroughly discussed in Subsection III-C and then in Sections IV and V, (9)-(11) allow computing a wide set of sensitivities and their solution is robust with respect to noise and bad data. These features are not provided by the weighted least square problem discussed in Subsection III-B below. Equations (9)-(11) can also be readily included in a time-domain integration algorithm and solved together with the set of DAEs that describe the dynamics of the system. This is the implementation utilized in the simulations carried out in the paper.

The low computational burden of solving the linear set of equations (9)-(11) allows its implementation in practical real-world DSEs, as illustrated in Fig. 1. As the power system evolves in time, PMU devices measure the voltages at the network buses, $\bar{\boldsymbol{v}}_B(t)$, and return the estimated values for the bus frequencies $\tilde{\boldsymbol{\omega}}_{\rm B}(t)$. These are then collected by the state estimator, which estimates the synchronous machine rotor speeds $\boldsymbol{\omega}_{\rm G}^*(t)$ through the solution of (9)-(11). Finally, the estimated $\boldsymbol{\omega}_{\rm G}^*(t)$ can be used by the system operator to take control actions $\boldsymbol{u}(t)$ on the system.

The added value of (9)-(11) and, in general, of rotor speed estimation is the ability to monitor on-line the transient behavior of synchronous machines. This is a valuable information for TSOs and can be utilized, for example, for on-line transient stability corrective control; wide area monitoring and control; and model validation in off-line stability analysis.

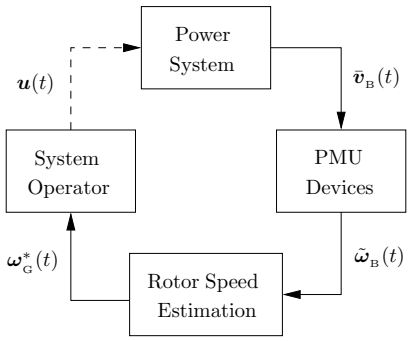

Fig. 1: Scheme of the proposed on-line frequency state estimator.

B. Weighted Least Square Problem

For the sake of comparison and the relevant topological properties that can be deduced from it, this subsection discusses the conventional linear measurement problem:

$$\Delta\tilde{\boldsymbol{\omega}}_{\rm B} + \boldsymbol{e}_{\rm B} = \mathbf{D}\Delta\boldsymbol{\omega}_{\rm G}, \tag{12}$$

whose optimal solution is:

$$\Delta\boldsymbol{\omega}_{\rm G}^* = (\mathbf{D}^T\mathbf{W}\mathbf{D})^{-1}\mathbf{D}^T\mathbf{W}\Delta\tilde{\boldsymbol{\omega}}_{\rm B} . \tag{13}$$

Assuming that the diagonal elements of $\mathbf{W}$ are equal, i.e., all PMUs are based on the same technology, the solution of (13) reduces to that of a linear least square problem:

$$\Delta\boldsymbol{\omega}_{\rm G}^* = (\mathbf{D}^T\mathbf{D})^{-1}\mathbf{D}^T\Delta\tilde{\boldsymbol{\omega}}_{\rm B} = \mathbf{D}^+\Delta\tilde{\boldsymbol{\omega}}_{\rm B} , \tag{14}$$

where $\mathbf{D}^+$ is the Moore-Penrose pseudo-inverse, or *left inverse*, of $\mathbf{D}$, which is unique as $\mathbf{D}$ has rank m.[1] From (5), one has:

$$\mathbf{D}^+ = -(\mathbf{B}_{\rm BB}^{-1}\mathbf{B}_{\rm BG})^+ . \tag{15}$$

Then, utilizing the matrix equivalence $(\mathbf{AB})^+ = \mathbf{B}^+\mathbf{A}^{-1}$, with $\mathbf{A}$ square and invertible and $\mathbf{B}$ rectangular, we can rewrite the right-hand side of (15):

$$\mathbf{D}^+ = -\mathbf{B}_{\rm BG}^+(\mathbf{B}_{\rm BB}^{-1})^{-1} = -\mathbf{B}_{\rm BG}^+\mathbf{B}_{\rm BB} . \tag{16}$$

From the discussion of (5), we already know that $\mathbf{D}$ is dense as it is obtained from the inverse of $\mathbf{B}_{\rm BB}$. The pseudo-inverse of $\mathbf{D}$, however, is extremely sparse. This can be readily deduced from the observation of the structure of $\mathbf{B}_{\rm BG}$. The elements of $\mathbf{B}_{\rm BG}$, say b_{ij}, are non-zero only in the rows corresponding to the buses at which each synchronous machine is connected. Then, it is straightforward to show that the pseudo-inverse of $\mathbf{B}_{\rm BG}$ is:

$$\begin{aligned} \mathbf{B}_{\rm BG}^+ &= (\mathbf{B}_{\rm BG}^T\mathbf{B}_{\rm BG})^{-1}\mathbf{B}_{\rm BG}^T \\ \Rightarrow \quad b_{ji}^+ &= \frac{1}{b_{ij}^2}\cdot b_{ij} = \frac{1}{b_{ij}}, \quad \forall\, b_{ij} \neq 0 . \end{aligned} \tag{17}$$

[1]The interested reader can find in [22] an application of (14) to compute the frequency of the COI based on PMU measurements and the FDF.

For example, let assume that

$$\mathbf{B}_{\text{BG}} = \begin{bmatrix} 0 & b_{12} \\ 0 & 0 \\ b_{31} & 0 \end{bmatrix} ,$$

which represents a 3-bus grid with two machines connected to buses 1 and 3, respectively. Then, from (17), we obtain:

$$\begin{aligned} \mathbf{B}_{\text{BG}}^{+} &= \left(\begin{bmatrix} 0 & 0 & b_{31} \\ b_{12} & 0 & 0 \end{bmatrix} \begin{bmatrix} 0 & b_{12} \\ 0 & 0 \\ b_{31} & 0 \end{bmatrix} \right)^{-1} \begin{bmatrix} 0 & 0 & b_{31} \\ b_{12} & 0 & 0 \end{bmatrix} \\ &= \begin{bmatrix} 1/b_{31}^2 & 0 \\ 0 & 1/b_{12}^2 \end{bmatrix} \begin{bmatrix} 0 & 0 & b_{31} \\ b_{12} & 0 & 0 \end{bmatrix} \\ &= \begin{bmatrix} 0 & 0 & 1/b_{31} \\ 1/b_{12} & 0 & 0 \end{bmatrix} . \end{aligned}$$

Hence, $\mathbf{B}_{\text{BG}}^{+}$ is as sparse as $\mathbf{B}_{\text{BG}}$ and is effectively the element-wise inverse of $\mathbf{B}_{\text{BG}}^{T}$. Non-zero elements of $\mathbf{B}_{\text{BG}}^{+}$ are in the columns corresponding to the buses at which each synchronous machine is connected. The product $\mathbf{B}_{\text{BG}}^{+}\mathbf{B}_{\text{BB}}$ and, hence, $\mathbf{D}^{+}$, have also the property that the number of non-zero elements of each row are equal to the first order connectivity degree of each synchronous machine terminal bus. This property has several relevant consequences, as follows.

- The non-zero elements of $\mathbf{D}^{+}$ indicate the minimum number of PMUs that have to be installed and at which buses.
- Each rotor speed can be estimated independently from the others, i.e., each row of $\mathbf{D}^{+}$ allows estimating one rotor speed.
- The minimum set of measurements required to estimate a rotor speed consists of only the measurements at the machine bus and its neighboring buses (see Fig. 2.b).
- A corollary of the above is that no less than two bus frequency measurements are needed to estimate the rotor speed of a machine connected to the system (see Fig. 2.a).
- It is also possible to actually need less measurements than twice the number of machines (see Fig. 2.c).

The latter three properties are relevant for large networks, as only a few local measurements are needed per machine. Moreover, given that the vast majority of power plants of real-world networks is connected in antenna to the rest of the system, the minimum number of bus frequency measurements required to estimate all rotor speeds is about twice the number of power plants.

The non-zero pattern of $\mathbf{D}^{+}$ shows that each rotor speed estimation in (14) is fully decoupled. It is thus possible to reformulate (6)-(7) as a set of m decoupled (decentralized) problems, each of which returns a single rotor speed. The main issue of (14), however, is that it does not provide any redundancy. $\mathbf{D}^{+}$ indicates the minimum number of required bus frequency measurements. All other measurements are redundant and improve the robustness of the solution of (6)-(7) but increase the "centralization" and the computational burden of the estimation problem. Also, remote measurements can be affected by delays. In practical applications, thus, one should find a trade-off between the simplicity of (14) and the robustness of (6)-(7). This point is duly discussed in Section V.

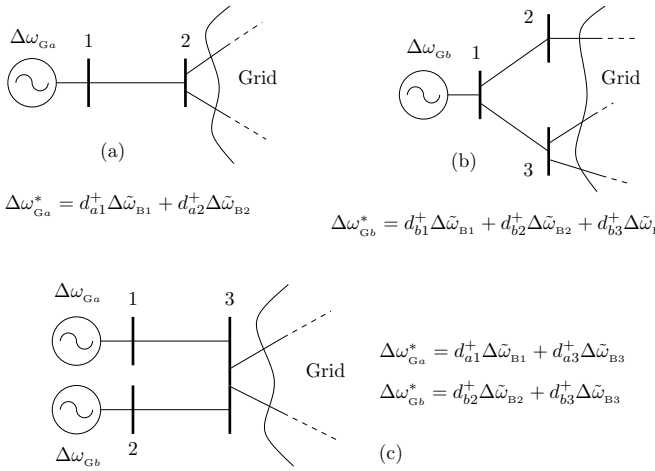

Fig. 2: Examples of synchronous machines connectivity: (a) antenna; (b) single machine connected to multiple buses; (c) multiple machines connected a the same bus. d_{ij}^{+} are the non-zero elements of $\mathbf{D}^{+}$.

C. Sensitivities

A relevant byproduct of solving an optimization problem is the ability to calculate with no extra computational effort the sensitivities of *everything with respect to everything*. This property relies on the dual variables and has already had a variety of applications in mathematical programming [23]–[25] as well as in the analysis of power system operation [26], [27] and state estimation [28].

To obtain the sensitivities of the convex problem (6)-(7), we proceed as in [28]. In this case, however, the procedure is quite straightforward as the starting optimization problem is convex quadratic. First, let differentiate the objective function (6) and the optimality conditions (9)-(11) with respect to the optimal values of the objective function and the solution (primal and dual), and the input bus frequency vector, namely $(J^*, \boldsymbol{\omega}_{\text{G}}^*, \boldsymbol{e}_{\text{B}}^*, \boldsymbol{\mu}_{\text{B}}^*, \tilde{\boldsymbol{\omega}}_{\text{B}})$:

$$0 = -dJ + \boldsymbol{e}_{\text{B}}^{*T}\mathbf{W}d\boldsymbol{e}_{\text{B}} , \tag{18}$$

$$\mathbf{0}_{m,1} = -\mathbf{B}_{\text{BG}}^{T}d\boldsymbol{\mu}_{\text{B}} , \tag{19}$$

$$\mathbf{0}_{n,1} = \mathbf{W}d\boldsymbol{e}_{\text{B}} - \mathbf{B}_{\text{BB}}^{T}d\boldsymbol{\mu}_{\text{B}} , \tag{20}$$

$$\mathbf{0}_{n,1} = -\mathbf{B}_{\text{BG}}d\boldsymbol{\omega}_{\text{G}} - \mathbf{B}_{\text{BB}}d\boldsymbol{e}_{\text{B}} - \mathbf{B}_{\text{BB}}d\tilde{\boldsymbol{\omega}}_{\text{B}} , \tag{21}$$

or, equivalently:

$$\mathbf{0}_{p,1} = \left[\begin{array}{c|c|c|c|c} -1 & \mathbf{0}_{1,m} & \boldsymbol{e}_{\text{B}}^{*T}\mathbf{W} & \mathbf{0}_{1,n} & \mathbf{0}_{1,n} \\ \hline \mathbf{0}_{m,1} & \mathbf{0}_{m,m} & \mathbf{0}_{m,n} & -\mathbf{B}_{\text{BG}}^{T} & \mathbf{0}_{m,n} \\ \hline \mathbf{0}_{n,1} & \mathbf{0}_{n,m} & \mathbf{W} & -\mathbf{B}_{\text{BB}}^{T} & \mathbf{0}_{n,n} \\ \hline \mathbf{0}_{n,1} & -\mathbf{B}_{\text{BG}} & -\mathbf{B}_{\text{BB}} & \mathbf{0}_{n,n} & -\mathbf{B}_{\text{BB}} \end{array}\right] \begin{bmatrix} dJ \\ d\boldsymbol{\omega}_{\text{G}} \\ d\boldsymbol{e}_{\text{B}} \\ d\boldsymbol{\mu}_{\text{B}} \\ d\tilde{\boldsymbol{\omega}}_{\text{B}} \end{bmatrix}, \tag{22}$$

where $p = m + 2n + 1$. The sensitivities with respect to the vector of measured bus frequencies $\boldsymbol{\omega}_{\text{B}}$ can be written as

$$\mathbf{U}\begin{bmatrix} dJ & d\boldsymbol{\omega}_{\text{G}} & d\boldsymbol{e}_{\text{B}} & d\boldsymbol{\mu}_{\text{B}} \end{bmatrix}^{T} = \mathbf{S}\, d\tilde{\boldsymbol{\omega}}_{\text{B}} , \tag{23}$$

where

$$\mathbf{U} = \left[\begin{array}{c|c|c|c} -1 & \mathbf{0}_{1,m} & \boldsymbol{e}_{\text{B}}^{*T}\mathbf{W} & \mathbf{0}_{1,n} \\ \hline \mathbf{0}_{m,1} & \mathbf{0}_{m,m} & \mathbf{0}_{m,n} & -\mathbf{B}_{\text{BG}}^{T} \\ \hline \mathbf{0}_{n,1} & \mathbf{0}_{n,m} & \mathbf{W} & -\mathbf{B}_{\text{BB}}^{T} \\ \hline \mathbf{0}_{n,1} & -\mathbf{B}_{\text{BG}} & -\mathbf{B}_{\text{BB}} & \mathbf{0}_{n,n} \end{array}\right], \tag{24}$$

and

$$\mathbf{S} = -\begin{bmatrix}\mathbf{0}_{1,n} & \mathbf{0}_{m,n} & \mathbf{0}_{n,n} & -\mathbf{B}_{\text{BB}}\end{bmatrix}^T . \quad (25)$$

Then one has:

$$\begin{bmatrix} dJ & d\boldsymbol{\omega}_{\text{G}} & d\boldsymbol{e}_{\text{B}} & d\boldsymbol{\mu}_{\text{B}}\end{bmatrix}^T = \mathbf{U}^{-1}\mathbf{S}\, d\tilde{\boldsymbol{\omega}}_{\text{B}} , \quad (26)$$

from which one can obtain the sensitivities of all primal and dual variables with respect to $\boldsymbol{\omega}_{\text{B}}$:

$$\begin{bmatrix} \frac{\partial J}{\partial \tilde{\boldsymbol{\omega}}_{\text{B}}} & \frac{\partial \boldsymbol{\omega}_{\text{G}}}{\partial \tilde{\boldsymbol{\omega}}_{\text{B}}} & \frac{\partial \boldsymbol{e}_{\text{B}}}{\partial \tilde{\boldsymbol{\omega}}_{\text{B}}} & \frac{\partial \boldsymbol{\mu}_{\text{B}}}{\partial \tilde{\boldsymbol{\omega}}_{\text{B}}}\end{bmatrix}^T = \mathbf{U}^{-1}\mathbf{S} . \quad (27)$$

For example, from (27), one can obtain:

$$\frac{\partial \boldsymbol{\omega}_{\text{G}}}{\partial \tilde{\boldsymbol{\omega}}_{\text{B}}} = -[\mathbf{B}_{\text{BG}}^T \mathbf{H} \mathbf{B}_{\text{BG}}]^{-1} \mathbf{B}_{\text{BG}}^T \mathbf{H} \mathbf{B}_{\text{BB}} , \quad (28)$$

where $\mathbf{H} = (\mathbf{B}_{\text{BB}} \mathbf{W}^{-1} \mathbf{B}_{\text{BB}}^T)^{-1}$. Equation (28) is consistent with (13). This can be shown by exploiting the following matrix properties:

- $(\mathbf{ABC})^{-1} = \mathbf{C}^{-1}\mathbf{B}^{-1}\mathbf{A}^{-1}$;
- $(\boldsymbol{A}^T)^{-1} = (\mathbf{A}^{-1})^T$;
- $(\boldsymbol{A}^{-1})^{-1} = \mathbf{A}$; and
- $(\mathbf{AB})^T = \mathbf{B}^T\mathbf{A}^T$

Then matrix $\mathbf{H}$ can be rewritten as:

$$\begin{aligned}\mathbf{H} &= (\mathbf{B}_{\text{BB}} \mathbf{W}^{-1} \mathbf{B}_{\text{BB}}^T)^{-1} = (\mathbf{B}_{\text{BB}}^T)^{-1} (\mathbf{W}^{-1})^{-1} \mathbf{B}_{\text{BB}}^{-1} \\ &= (\mathbf{B}_{\text{BB}}^{-1})^T \mathbf{W} \mathbf{B}_{\text{BB}}^{-1} ,\end{aligned} \quad (29)$$

and, substituting the obtained expression into (28), we obtain:

$$\begin{aligned}\frac{\partial \boldsymbol{\omega}_{\text{G}}}{\partial \tilde{\boldsymbol{\omega}}_{\text{B}}} &= -[\mathbf{B}_{\text{BG}}^T (\mathbf{B}_{\text{BB}}^{-1})^T \mathbf{W} \mathbf{B}_{\text{BB}}^{-1} \mathbf{B}_{\text{BG}}]^{-1} \mathbf{B}_{\text{BG}}^T (\mathbf{B}_{\text{BB}}^{-1})^T \mathbf{W} \mathbf{B}_{\text{BB}}^{-1} \mathbf{B}_{\text{BB}} \\ &= -[(\mathbf{B}_{\text{BB}}^{-1} \mathbf{B}_{\text{BG}})^T \mathbf{W} \mathbf{B}_{\text{BB}}^{-1} \mathbf{B}_{\text{BG}}]^{-1} (\mathbf{B}_{\text{BB}}^{-1} \mathbf{B}_{\text{BG}})^T \mathbf{W},\end{aligned} \quad (30)$$

which, recalling the definition of $\mathbf{D}$ in (5), namely $\mathbf{D} = -\mathbf{B}_{\text{BB}}^{-1}\mathbf{B}_{\text{BG}}$, is the same expression that can be obtained by differentiating (13) with respect to $\tilde{\boldsymbol{\omega}}_{\text{B}}$ and $\boldsymbol{\omega}_{\text{G}}^*$.

Another relevant sensitivity vector that can be obtained from (27) is $\frac{\partial J}{\partial \tilde{\boldsymbol{\omega}}_{\text{B}}}$. Since the manipulation of (27) is rather involved, we determine such sensitivities as follows. First, observe that, from (18):

$$\frac{\partial J}{\partial \boldsymbol{e}_{\text{B}}} = \boldsymbol{e}_{\text{B}}^{*T} \mathbf{W} . \quad (31)$$

Then, from (10), one obtains:

$$\boldsymbol{e}_{\text{B}}^{*T} \mathbf{W} = \boldsymbol{\mu}_{\text{B}}^{*T} \mathbf{B}_{\text{BB}} , \quad (32)$$

where we have used the well-known property $(\mathbf{A}^T\mathbf{B})^T = \mathbf{B}^T\mathbf{A}$. Then, multiplying (21) by $\boldsymbol{\mu}_{\text{B}}^{*T}$ and observing from (9) that $\boldsymbol{\mu}_{\text{B}}^{*T} \mathbf{B}_{\text{BG}} = \mathbf{0}_{1,m}$, one has:

$$\frac{\partial \boldsymbol{e}_{\text{B}}}{\partial \tilde{\boldsymbol{\omega}}_{\text{B}}} = -\mathbf{1}_{n,1} . \quad (33)$$

Finally, multiplying together (31) and (33), imposing (32) and applying the chain rule, lead to the sought expression:

$$\frac{\partial J}{\partial \tilde{\boldsymbol{\omega}}_{\text{B}}} = \frac{\partial J}{\partial \boldsymbol{e}_{\text{B}}} \frac{\partial \boldsymbol{e}_{\text{B}}}{\partial \tilde{\boldsymbol{\omega}}_{\text{B}}} = -\boldsymbol{e}_{\text{B}}^{*T} \mathbf{W} = -\boldsymbol{\mu}_{\text{B}}^{*T} \mathbf{B}_{\text{BB}} . \quad (34)$$

The significance of the sensitivites determined in this section is shown in the illustrative example and the case study below. Such sensitivities can also be utilized to identify the buses whose frequency measurements improve the robustness of the rotor speed estimation. This topic is beyond the scope of this paper and will be the object of future work.

IV. Illustrative Example

This section presents an illustrative example based on the WSCC 9-bus system shown in Fig. 3. This network includes three synchronous machines, loads and transformers, and six transmission lines, as well as primary frequency and voltage regulation. The interested reader can find all data in [32].

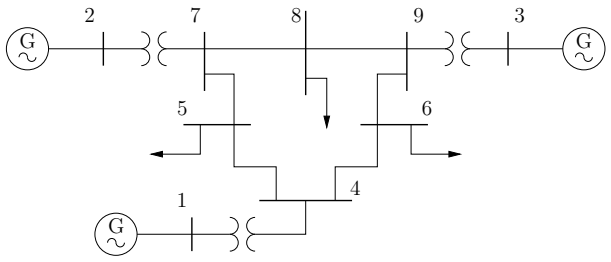

Fig. 3: WSCC 9-bus system utilized in the illustrative example.

In this example, one PMU is installed at every bus of the network. It is assumed that all PMU devices are based on the same technology and have same measurement standard deviations, namely, $\sigma_i = 10^{-3}$, $\forall i = 1, \ldots, 9$. Hence, $\mathbf{W} = 10^6 \cdot \mathbf{I}_9$. Matrices $\mathbf{B}_{\text{BB}}$, $\mathbf{B}_{\text{BG}}$ and $\mathbf{D}$ for the WSCC 9-bus system are shown in Tables I, II and III, respectively.

TABLE I: Matrix $\mathbf{B}_{\text{BB}}$ for the WSCC 9-bus system.

Bus #	Bus #								
	1	2	3	4	5	6	7	8	9
1	-30.04	0	0	17.36	0	0	0	0	0
2	0	-22.32	0	0	0	0	16.00	0	0
3	0	0	-21.70	0	0	0	0	0	17.06
4	17.36	0	0	-39.31	11.60	10.51	0	0	0
5	0	0	0	11.60	-17.34	0	5.975	0	0
6	0	0	0	10.51	0	-15.84	0	0	5.588
7	0	16.00	0	0	5.975	0	-35.45	13.70	0
8	0	0	0	0	0	0	13.70	-23.30	9.784
9	0	0	17.06	0	0	5.588	0	9.784	-32.15

TABLE II: Matrix $\mathbf{B}_{\text{BG}}^T$ for the WSCC 9-bus system.

Gen. #	Bus #								
	1	2	3	4	5	6	7	8	9
1	12.682	0	0	0	0	0	0	0	0
2	0	6.315	0	0	0	0	0	0	0
3	0	0	4.637	0	0	0	0	0	0

From the structure of $\mathbf{B}_{\text{BG}}$, it is relevant to observe that the dual variables $\boldsymbol{\mu}_{\text{B}}$ are always null at the generation buses. Matrix $\mathbf{B}_{\text{BG}}$, in fact, has non-null elements only in the columns corresponding to the buses where generators are connected. The optimality condition (9) for the WSCC 9-bus system gives:

$$0 = 12.682\, \mu_{\text{B1}}^*, \quad 0 = 6.315\, \mu_{\text{B2}}^*, \quad 0 = 4.637\, \mu_{\text{B3}}^* . \quad (35)$$

Then, Lagrangian multipliers $\boldsymbol{\mu}_{\text{B}}$ are non-null only at load or transition buses.

The sensitivities $\partial \boldsymbol{\omega}_{\text{G}} / \partial \tilde{\boldsymbol{\omega}}_{\text{B}}$, obtained from (28) are shown in Table IV. Since $\mathbf{W}$ is diagonal and all its diagonal elements are equal, the sensitivities do not depend on its values and, in this case, one has:

$$\frac{\partial \boldsymbol{\omega}_{\text{G}}}{\partial \tilde{\boldsymbol{\omega}}_{\text{B}}} = \mathbf{D}^+ . \quad (36)$$

TABLE III: Matrix $\mathbf{D}^T$ for the WSCC 9-bus system.

Gen. #	Bus # 1	2	3	4	5	6	7	8	9
1	0.8225	0.2510	0.2847	0.6928	0.5843	0.5874	0.3500	0.3578	0.3620
2	0.1249	0.6499	0.2327	0.2163	0.3211	0.2479	0.5118	0.4251	0.2959
3	0.1041	0.1708	0.5668	0.1801	0.2027	0.2780	0.2383	0.3287	0.4492

These sensitivities are constant if there is no change of the topology of the network. Note also that (36) can be obtained directly from differentiating (14).

As discussed in Subsection III-B, $\mathbf{D}^+$ is very sparse. In this example, the three machines are connected in antenna and, hence, at least 6 PMU measurements at buses 1-4, 7 and 9 are needed to estimate all rotor speeds.

TABLE IV: Sensitivities $\frac{\partial \omega_{\mathrm{G}}}{\partial \tilde{\omega}_{\mathrm{B}}} = \mathbf{D}^+$ for the WSCC 9-bus system

$\partial\omega_{Gi}$	$\partial\tilde{\omega}_{Bj}$ 1	2	3	4	5	6	7	8	9
1	2.369	0	0	-1.369	0	0	0	0	0
2	0	3.534	0	0	0	0	-2.534	0	0
3	0	0	4.680	0	0	0	0	0	-3.680

We next analyze the sensitivities $\frac{\partial J}{\partial \tilde{\omega}_{\mathrm{B}}}$ which are given by (34). For the sake of example, we consider the sensitivity at the generator bus 1, namely $\frac{\partial J}{\partial \tilde{\omega}_{\mathrm{B1}}}$, and the sensitivity at load bus 8, namely, $\frac{\partial J}{\partial \tilde{\omega}_{\mathrm{B8}}}$. From (34), one has:

$$\begin{aligned} \frac{\partial J}{\partial \tilde{\omega}_{\mathrm{B1}}} &= 30.04\,\mu^*_{\mathrm{B1}} - 17.36\,\mu^*_{\mathrm{B4}} = -17.36\,\mu^*_{\mathrm{B4}}\,, \\ \frac{\partial J}{\partial \tilde{\omega}_{\mathrm{B8}}} &= -13.7\,\mu^*_{\mathrm{B7}} + 23.3\,\mu^*_{\mathrm{B8}} - 9.784\,\mu^*_{\mathrm{B9}}\,, \end{aligned} \tag{37}$$

where in the first of (34), we have imposed the condition $\mu^*_{\mathrm{B1}} = 0$ obtained from the first of (35). From (6) and again from (34), the sensitivities in (37) are equivalent to the expressions:

$$\begin{aligned} \frac{\partial J}{\partial \tilde{\omega}_{\mathrm{B1}}} &= -\frac{e^*_{\mathrm{B1}}}{\sigma^2_{\mathrm{B1}}} = -10^6 \cdot e^*_{\mathrm{B1}}\,, \\ \frac{\partial J}{\partial \tilde{\omega}_{\mathrm{B8}}} &= -\frac{e^*_{\mathrm{B8}}}{\sigma^2_{\mathrm{B8}}} = -10^6 \cdot e^*_{\mathrm{B8}}\,, \end{aligned} \tag{38}$$

which indicate that the sensitivities of the objective function with respect to the bus frequency measurements are inversely proportional to the variance of the measurements themselves.

Let consider the loss of load connected at bus 5 occurring at $t = 1$ s. Figure 4 shows the trajectory of the actual rotor speed $\hat{\omega}_{\mathrm{G1}}$ of the synchronous machine connected at bus 1; the estimated rotor speed ω^*_{G1} obtained by solving (9)-(11); and the error $|\hat{\omega}_{\mathrm{G1}} - \omega^*_{\mathrm{G1}}|$. Note that $\hat{\omega}_{\mathrm{G1}}$ is the state variable of the machine swing equation, which, in this paper, is obtained through the numerical integration of the system model. In real-life applications, however, $\hat{\omega}_{\mathrm{G1}}$ is actually not available to system operators (see also the scheme of Fig. 1). Along the time domain simulation, the bus measurements $\tilde{\boldsymbol{\omega}}_{\mathrm{B}}$ are obtained using PMU devices equipped with a synchronous reference-frame phase-locked loop [33].

No noise is considered in this example. The error between the ideal and the estimated rotor speeds is due exclusively to the PMU tracking. Apart from the first instants after the contingency, such an error is below 0.0002 pu, i.e., 0.012 Hz for a 60 Hz system and 0.01 Hz for a 50 Hz one.

The average error decreases as the rotor speed stabilizes after the contingency, thus leading to the conclusion that the average error is proportional to the rate of change of frequency. This is a consequence of the dynamic behaviour of the swing equations of synchronous machines. Following a contingency, the power imbalance in the grid accelerates or decelerates the machines, thus creating frequency variations, which are different from bus to bus and maximum in the first few seconds after the contingency. Then, the primary frequency controllers act on the turbine governors of the machines and help recover a synchronous condition, i.e., a condition in which the rotor speeds of the machines converge to a common value. In the first seconds after a contingency, thus, machine rotor speeds show the largest rate of change and, consequently, the highest estimation errors.

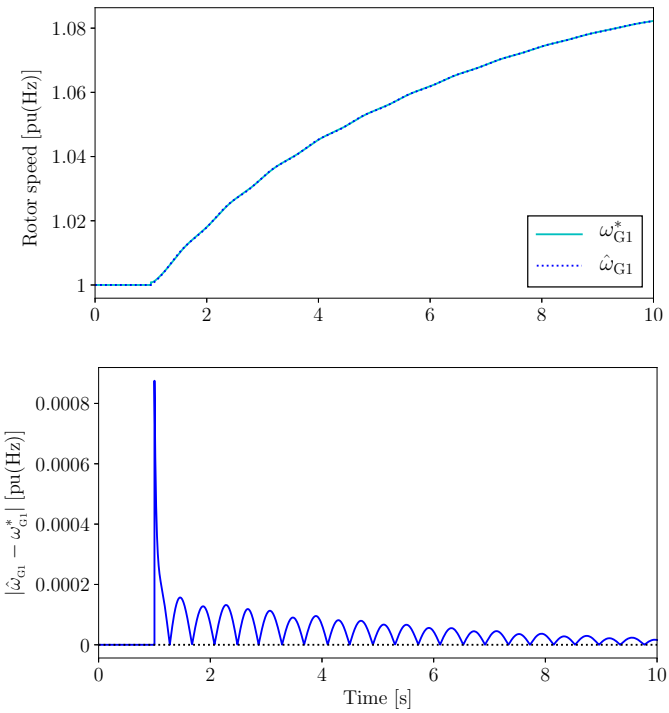

Fig. 4: Upper panel: Actual rotor speed $\hat{\omega}_{\mathrm{G1}}$ of the synchronous machine 1 and the estimated quantity ω^*_{G1}. Lower panel: Estimation error of the rotor speed of machine 1 for the WSCC 9-bus system.

Figure 5 shows the trajectories of the sensitivities $\partial J/\partial \tilde{\omega}_{\mathrm{B1}}$ and $\partial J/\partial \tilde{\omega}_{\mathrm{B8}}$ for the contingency discussed above. Similarly to the error between actual and estimated rotor speeds, the corresponding sensitivities decrease as the rate of change of frequency decreases. In steady-state all sensitivities $\partial J/\partial \tilde{\omega}_{\mathrm{B}i}$ are null, since the frequency is the same at every bus of the network.

Finally, we illustrate the formulation of the decoupled state estimation problem to determine a single rotor speed. Let consider $\Delta\omega_{\mathrm{G1}}$. Equation (14) and Table IV indicate that the minimum set of measurements required to estimate this

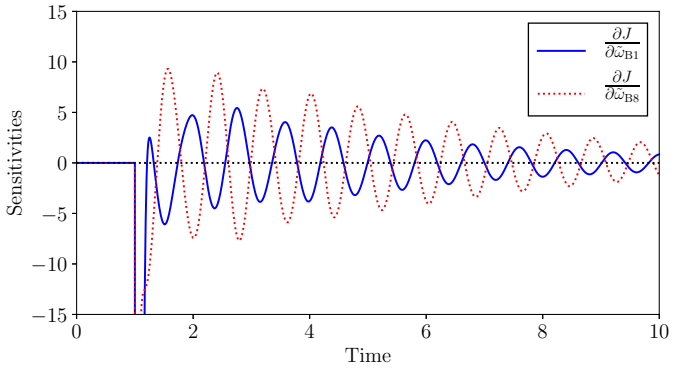

Fig. 5: Sensitivities $\partial J/\partial\tilde{\omega}_{B1}$ and $\partial J/\partial\tilde{\omega}_{B8}$ for the WSCC 9-bus system.

rotor speed are $\Delta\tilde{\omega}_{B1}$ and $\Delta\tilde{\omega}_{B4}$. The resulting state estimation problem is:

$$\begin{aligned} \min_{(e_{B1},e_{B4},\Delta\omega_{G1})} \quad & J = \frac{1}{2}\left(w_1 e_{B1}^2 + w_2 e_{B4}^2\right) \\ \text{s.t.} \quad & 0 = 12.682\,\Delta\omega_{G1} - 30.04\,(\Delta\tilde{\omega}_{B1} + e_{B1}) \\ & \quad + 17.36\,(\Delta\tilde{\omega}_{B4} + e_{B4}) \qquad : \mu_B \ . \end{aligned}$$

The KKT conditions lead to $e_{B1}^* = e_{B4}^* = \mu_B^* = 0$, and:

$$\Delta\omega_{G1}^* = 2.369\,\Delta\tilde{\omega}_{B1} - 1.369\,\Delta\tilde{\omega}_{B4} \ .$$

The latter can be directly obtained from (14). The full optimization problem (6)-(7) provides significantly more redundancy than (14), which is to be expected as (6)-(7) exploit a higher number of measurements. For example, if $\tilde{\omega}_{B4}$ is missing, the estimation provided by (14) is compromised, but one can still reconstruct $\tilde{\omega}_{B4}$ from $\tilde{\omega}_{B1}$, $\tilde{\omega}_{B5}$ and $\tilde{\omega}_{B6}$ (see the fourth row of matrix $\mathbf{B}_{BB}$ in Table I). Figure 6 shows the estimation of ω_{G1}^* considering different sets of PMU measurements.

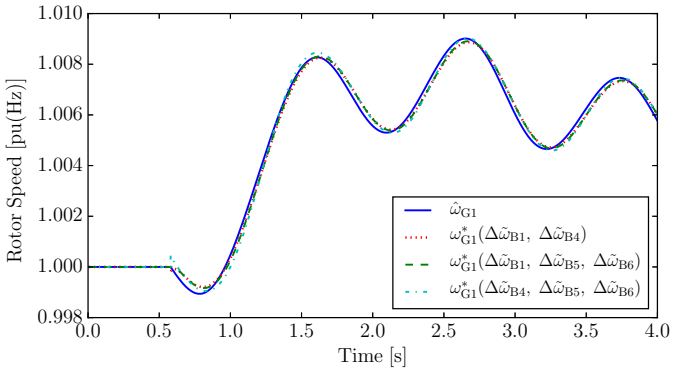

Fig. 6: Actual rotor speed $\tilde{\omega}_{G1}$ of the sync. machine 1 and the estimated quantity ω_{G1}^* considering different sets of PMU measurements.

V. Case Study

This section considers a dynamic model of the all-island Irish transmission system. The model includes 1,479 buses, 1,851 transmission lines and transformers, 245 loads, 22 conventional synchronous power plants modeled with 6th order synchronous machine models with d-axis saturation, AVRs and turbine governors; 6 PSSs; and 176 wind power plants, 34 of which are equipped with constant-speed and 142 with doubly-fed induction generators.

The topology and the steady-state data of the all-island Irish system are made available by the Irish TSO, EirGrid.[2] Dynamic data of generators and controllers, while guessed, have been determined case by case, based on power plant capacity and technology, in order to be as close as possible to the real-world Irish system. No load dynamic is considered. All simulations and plots presented in this section were obtained using the software tool Dome [34] running on a 4 core 2.60 GHz Intel© Core i7^{TM} with 8 GB of RAM.

Four scenarios are considered in the case study. In Subsection V-A, the sensitivities $\partial\omega_G/\partial\tilde{\omega}_B$ of the Irish system are analyzed. Subsection V-B studies the robustness of both estimation approaches against the loss of some key PMU measurements. Finally, Subsections V-C and V-D compare the sensitivity of the optimization problem (OPT) (6)-(7) and the WLS estimation techniques considering noise and latency in the PMU signals $\Delta\tilde{\omega}_B$, respectively. In the following subsections, due to space limitation, we show the results only for one machine. Results obtained for all other machines are similar in terms of both accuracy and sensitivity to bad data, noise and latency.

The contingency considered in all scenarios is a three-phase fault occurring at $t = 1$ s, and cleared after 150 ms by disconnecting the corresponding line. We wish to emphasize that the proposed frequency estimation is particularly relevant for the very first few seconds following severe events that trigger electromechanical oscillations of the machines. Only in this time frame and scenario, frequencies are different from bus to bus.

Due to the linear formulation, the high sparsity of all matrices involved, and the fact that no matrix factorization is required, the computational burden of the two problems is negligible. Solving the full OPT and WLS problems for the whole Irish system requires about 100 µs and 5 µs, respectively, per time step, on the platform indicated above. These times are orders of magnitude smaller than the phenomenon to be analyzed, i.e., synchronous machine electromechanical oscillations, and thus these problems are suited for implementation in real-life applications.

A. Sensitivity Analysis

In this subsection, we consider the sensitivities $\partial\omega_G/\partial\tilde{\omega}_B$. To this aim, matrix $\mathbf{D}^+$ is computed from (16). The submatrix of $\mathbf{D}^+$ including generator buses (columns) and neighboring buses (rows) is shown in Fig. 7.

Matrix $\mathbf{D}^+$ has only 44 non-zero elements over a total of 32,538, thus showing that, if measurement redundancy is neglected, one only needs a very reduced set of PMU measurements to estimate the rotor speeds of all synchronous machines, even for large systems. For the Irish system, in fact, the minimum set includes 42 PMUs, as two pairs of machines are connected with the topology depicted in Fig. 2.c.

[2]See webpage: `http://www.eirgridgroup.com/`

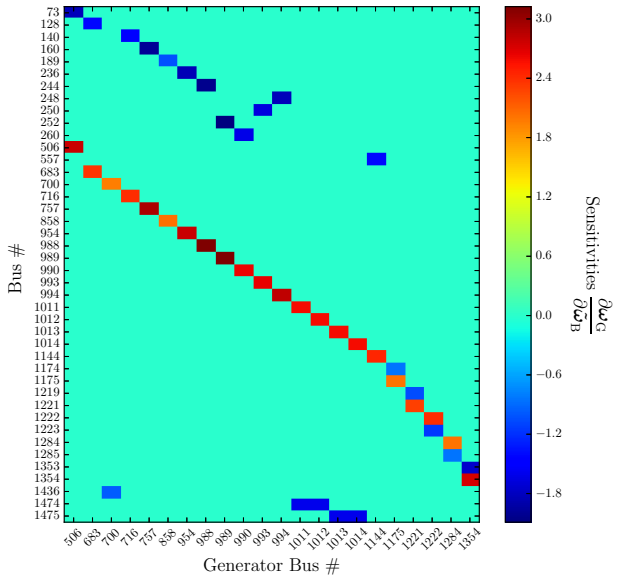

Fig. 7: Sensitivities $\partial\omega_{\mathrm{G}}/\partial\tilde{\omega}_{\mathrm{B}}$ for the Irish system.

B. Measurement Redundancy and Robustness

The robustness against the loss of one of the measurement signals of the two proposed estimation approaches is studied next. In this scenario, the accuracy of each approach is compared when estimating the rotor speed of a synchronous machine connected to the system as in Fig. 2.a when a large transient occurs in the system, and one of the two PMUs fails to send the measurement $\tilde{\omega}_{\mathrm{B},i}$. The accuracy of the OPT and WLS problems assuming that all PMU measurements are available is shown in Fig. 8.

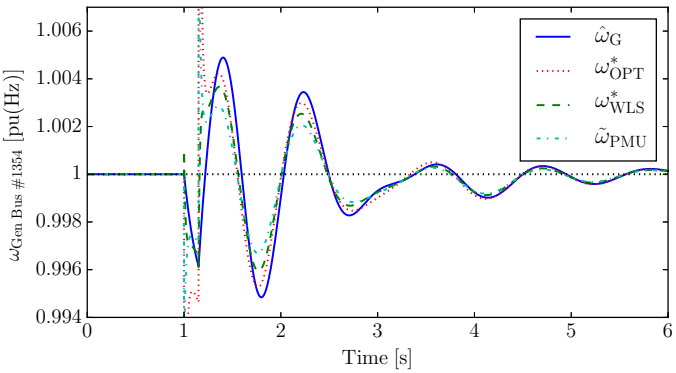

Fig. 8: Actual rotor speed ($\hat{\omega}_{\mathrm{G}}$) and estimated ($\omega^*_{\mathrm{OPT}}$ and ω^*_{WLS}) of a synchronous machine of the Irish system, and PMU frequency measurement at the machine bus ($\tilde{\omega}_{\mathrm{PMU}}$).

Both techniques are able to capture the machine rotor speed variations with better accuracy than the measurement provided by the PMU connected at the machine bus. The OPT estimation is slightly better than that obtained with the WLS. The total amplitude of the characteristic spikes of the PMU during the discontinuous events (fault and line outage), and the consequent spikes of the estimation techniques, is not shown in order to better capture the more relevant electromechanical oscillations.

To study the impact of a PMU malfunction, it is assumed that $\Delta\tilde{\omega}_{\mathrm{B},i} = 0$ from the beginning of the simulation, and results are shown in Fig. 9.

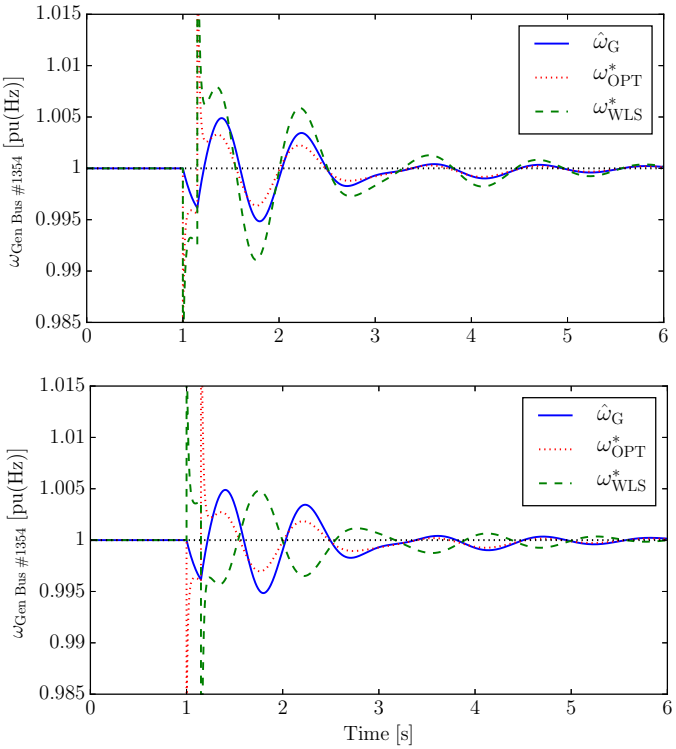

Fig. 9: Actual rotor speed ($\hat{\omega}_{\mathrm{G}}$) and estimated ($\omega^*_{\mathrm{OPT}}$ and ω^*_{WLS}) of a synchronous machine of the Irish system. Upper panel: Failure of PMU at machine neighboring bus. Lower panel: Failure of PMU at machine bus.

In the two cases simulated, namely the failure of the PMU at the machine neighboring bus (Fig. 9.a), and at the machine bus (Fig. 9.b), the measurement redundancy of the OPT problem allows correcting the erroneous $\tilde{\omega}_{\mathrm{B},i}$, thus providing a highly accurate estimation of $\hat{\omega}_{\mathrm{G}}$. Bad data considerably impact on the WLS-based estimation, in particular if the bad signal is that of the PMU at the machine bus, where the estimation is in counter-phase with the actual $\hat{\omega}_{\mathrm{G}}$.

C. Noise

The last scenario studies the sensitivity of the two estimation approaches to the presence of noise in the input signals of the PMUs. The noise is modeled as an Ornstein-Uhlenbeck's process with Gaussian distribution is applied to all bus voltage phase angles [35]. The noisy time-varying voltages are then utilized as input signals to the Phase-Locked Loop (PLL) of the PMUs that measure bus frequencies (see the Appendix for the PLL model). Results are depicted in Fig. 10. As expected, the OPT problem shows a lower sensitivity to noise than the WLS. The OPT problem, in fact, can include more measurements than the WLS problem. The higher the number

of measurements, the lower the impact of measurement errors on the estimation of rotor speeds.

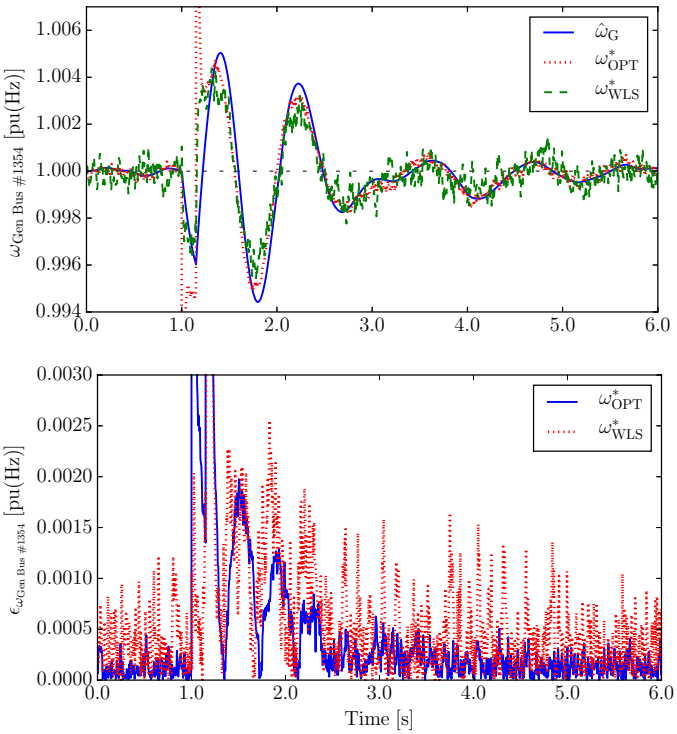

Fig. 10: Actual rotor speed ($\hat{\omega}_G$) and estimated (ω^*_{OPT} and ω^*_{WLS}) of a synchronous machine of the Irish system under the presence of noise. Upper panel: Trajectories. Lower panel: Absolute errors of the estimation.

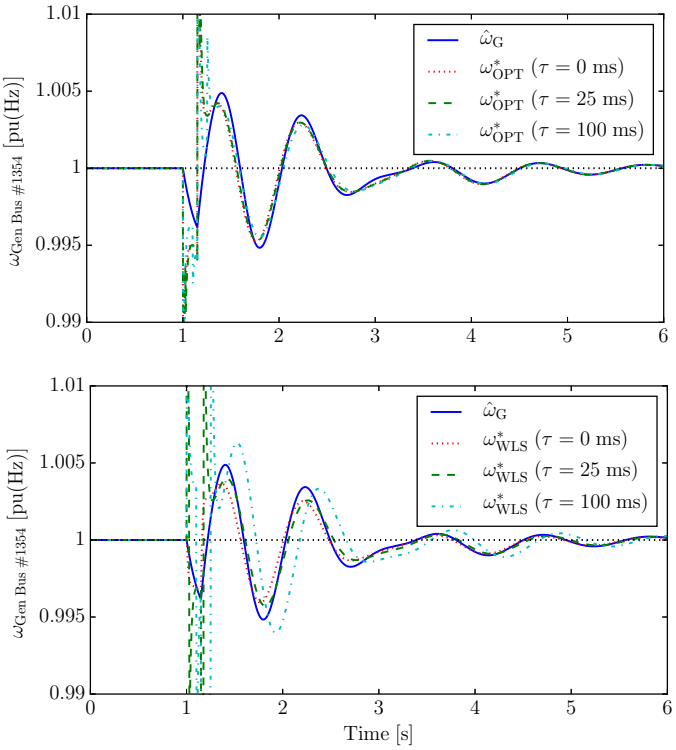

Fig. 11: Actual rotor speed ($\hat{\omega}_G$) and estimates (ω^*_{OPT} and ω^*_{WLS}) for a synchronous machine of the Irish system with latency in the PMU signal of the synchronous machine bus. Upper panel: Optimization problem. Lower panel: Weighted Least Square.

D. Latency

Latency is modeled as a constant delay that is introduced in the PLL output signals of the PMUs that provide bus frequency measurements. Each delay is composed of a term due to the measurement process plus a communication delay in transmitting the signal to the control center. In the simulations, we consider only a difference in communication delays, τ, between PMUs and, hence, the latency is applied to all but one PMUs involved in the estimation of each rotor speed. Two cases are considered, namely τ = 25 ms (short distance) and τ = 100 ms (long distance). Results are shown in Figs. 11 (τ in the signal of the machine bus) and 12 (τ in the signal of the machine neighboring bus).

Regarding the scenario involving noise, the OPT problem shows good robustness with respect to measurement latencies, regardless of the affected PMU and the value of τ. The WLS is more sensitive to latency. WLS accuracy is compromised if τ = 100 ms and shows significantly more and larger spikes than the OPT.

E. Remarks on Simulation Results

Simulation results for the all-island Irish system indicate that the OPT shows a fairly good accuracy of its estimation. It also shows a high robustness against the malfunctioning of PMU devices, and a low sensitivity to the presence of noise and latency in the PMU measured signals. The rotor speed of a given machine, in fact, can be estimated with a good approximation even if no PMU measurement at the machine bus is available.

The WLS approach based on the pseudo-inverse of the FDF matrix indicates that only 42 PMUs are required for the considered model of the all-island Irish system and provides the location of such measurements. The WLS approach minimizes the computational burden and shows that the implementation the rotor speed estimation is viable in practice. However, due to the reduced number of measurements, this approach tends to be sensitive to bad data, noise and latency. Note, however, that the impact of noise and latency can be reduced through appropriate filtering and/or compensation techniques, as stated, e.g., in [36].

VI. Conclusions

The paper proposes a linear, model-agnostic optimization problem that estimates the rotor speeds of synchronous machines based on the FDF and PMU frequency measurements. The paper also provides all sensitivities of the proposed optimization problem as well as an analytical expression of the conventional WLS problem, that gives the minimum set of PMU measurements required to estimate rotor speeds. Such a minimum set also allows implementing a fully decentralized state estimation. The decentralized problem, however, gives up redundancy and is less robust than the full optimization problem. Real-world implementation of the proposed DSE have

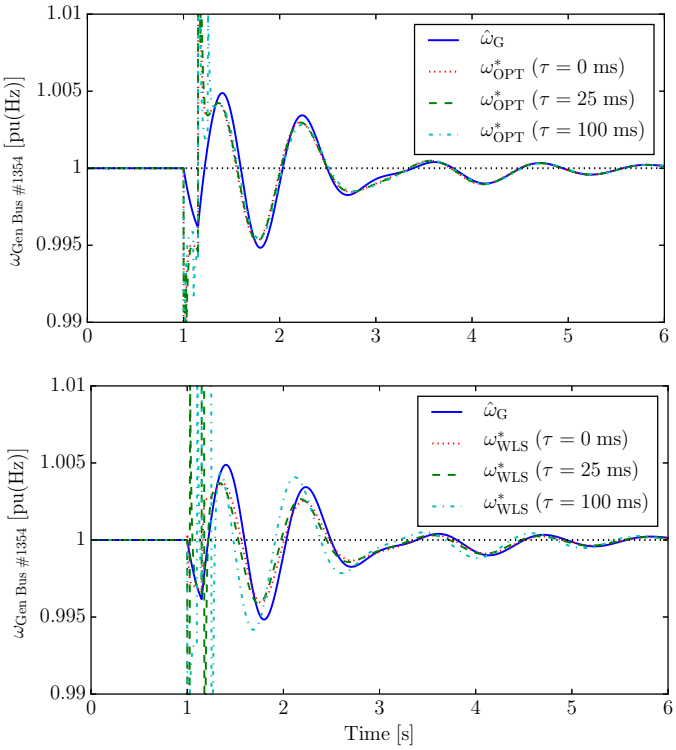

Fig. 12: Actual rotor speed ($\hat{\omega}_{\text{G}}$) and estimates (ω^*_{OPT} and ω^*_{WLS}) for a synchronous machine of the Irish system with latency in the PMU signal of the machine neighboring bus. Upper panel: Optimization problem. Lower panel: Weighted Least Square.

thus to find a tradeoff between the robustness of the optimization problem and the low requirements and decentralization of the WLS approach.

Future work will focus on studying the effect of system parameter inaccuracies on the performance of the rotor-speed estimation technique. We will also study how to improve the robustness of the proposed optimization problem through, for example, an EKF technique and consider practical implementation aspects, such as communication issues of PMU data.

APPENDIX

The synchronous reference frame phase-locked loop (SRF-PLL) is one of the simplest and most commonly used PLLs configurations [20], [37]. A fundamental-frequency model of a SRF is depicted in Fig. 13, where the phase detector (PD) is modeled as lag transfer function; the loop filter (LF) is a PI controller; and the voltage-controlled oscillator (VCO) is implemented as an integrator. In this scheme, v_q is the q-axis component of the bus voltage and $\hat{v}_q$ is the corresponding estimated quantity. The output of the LF is an estimation of the frequency deviation $\Delta\hat{\omega}$ at the bus.

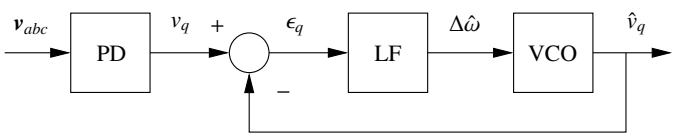

Fig. 13: Scheme of the SRF-PLL.

REFERENCES

[1] C. K. Gharban and B. J. Cory, "Non-linear dynamic power system state estimation," *IEEE Trans. on Power Systems*, vol. 1, no. 3, pp. 276–283, Aug 1986.

[2] S. J. Huang and K. R. Shih, "Dynamic-state-estimation scheme including nonlinear measurement-function considerations," *IEE Procs on Gen., Transm. and Distr.*, vol. 149, no. 6, pp. 673–678, Nov 2002.

[3] H. M. Beides and G. T. Heydt, "Dynamic state estimation of power system harmonics using Kalman filter methodology," *IEEE Trans. on Power Delivery*, vol. 6, no. 4, pp. 1663–1670, Oct 1991.

[4] Z. Huang, K. Schneider, and J. Nieplocha, "Feasibility studies of applying Kalman filter techniques to power system dynamic state estimation," in *Procs of the IPEC*, Dec 2007, pp. 376–382.

[5] N. Zhou, D. Meng, and S. Lu, "Estimation of the dynamic states of synchronous machines using an extended particle filter," *IEEE Trans. on Power Systems*, vol. 28, no. 4, pp. 4152–4161, Nov 2013.

[6] H. Bilil and H. Gharavi, "Mmse-based analytical estimator for uncertain power system with limited number of measurements," *IEEE Trans. on Power Systems*, pp. 1–1, 2018.

[7] L. Zhao and A. Abur, "Multi area state estimation using synchronized phasor measurements," *IEEE Trans. on Power Systems*, vol. 20, no. 2, pp. 611–617, May 2005.

[8] S. Mohagheghi, R. H. Alaileh, G. Cokkinides, and A. P. S. Meliopoulos, "Distributed state estimation based on the supercalibrator concept - laboratory implementation," in *Procs of the IREP Symposium*, Aug 2007, pp. 1–9.

[9] E. Ghahremani and I. Kamwa, "Dynamic state estimation in power system by applying the extended Kalman filter with unknown inputs to phasor measurements," *IEEE Trans. on Power Systems*, vol. 26, no. 4, pp. 2556–2566, Nov 2011.

[10] ——, "Online state estimation of a synchronous generator using unscented Kalman filter from phasor measurements units," *IEEE Trans. on Energy Conversion*, vol. 26, no. 4, pp. 1099–1108, Dec 2011.

[11] Z. Huang, P. Du, D. Kosterev, and S. Yang, "Generator dynamic model validation and parameter calibration using phasor measurements at the point of connection," *IEEE Trans. on Power Systems*, vol. 28, no. 2, pp. 1939–1949, May 2013.

[12] E. Farantatos, G. K. Stefopoulos, G. J. Cokkinides, and A. P. Meliopoulos, "PMU-based dynamic state estimation for electric power systems," in *Procs of the IEEE PES General Meeting*, July 2009, pp. 1–8.

[13] S. Wang, W. Gao, and A. P. S. Meliopoulos, "An alternative method for power system dynamic state estimation based on unscented transform," *IEEE Trans. on Power Systems*, vol. 27, no. 2, pp. 942–950, May 2012.

[14] A. Rouhani and A. Abur, "Linear phasor estimator assisted dynamic state estimation," *IEEE Trans. on Smart Grid*, vol. 9, no. 1, pp. 211–219, Jan 2018.

[15] A. K. Singh and B. C. Pal, "Decentralized dynamic state estimation in power systems using unscented transformation," *IEEE Trans. on Power Systems*, vol. 29, no. 2, pp. 794–804, March 2014.

[16] N. Zhou, D. Meng, Z. Huang, and G. Welch, "Dynamic state estimation of a synchronous machine using PMU data: A comparative study," *IEEE Trans. on Smart Grid*, vol. 6, no. 1, pp. 450–460, Jan 2015.

[17] E. Ghahremani and I. Kamwa, "Local and wide-area PMU-based decentralized dynamic state estimation in multi-machine power systems," *IEEE Trans. on Power Systems*, vol. 31, no. 1, pp. 547–562, Jan 2016.

[18] F. Milano and Á. Ortega, "Frequency divider," *IEEE Trans. on Power Systems*, vol. 32, no. 2, pp. 1493–1501, March 2017.

[19] Á. Ortega and F. Milano, "Comparison of bus frequency estimators for power system transient stability analysis," in *Procs of the POWERCON*, Wollongong, Australia, Sep 2016.

[20] ——, "Impact of frequency estimation for VSC-based devices with primary frequency control," in *Procs of the ISGT Europe Conf.*, Torino, Italy, Sep 2017.

[21] J. Zhao, L. Mili, and F. Milano, "Robust frequency divider for power system online monitoring and control," *IEEE Trans. on Power Systems*, vol. PP, no. 99, pp. 1–1, 2017.

[22] F. Milano, "Rotor speed-free estimation of the frequency of the center of inertia," *IEEE Trans. on Power Systems*, vol. 33, no. 1, pp. 1153–1155, Jan 2018.

[23] E. Castillo, A. S. Hadi, A. Conejo, and A. Fernández-Canteli, "A general method for local sensitivity analysis with application to regression models and other optimization problems," *Technometrics*, vol. 46, no. 4, pp. 430–444, 2004.

[24] E. Castillo, A. J. Conejo, C. Castillo, R. Mínguez, and D. Ortigosa, "Perturbation approach to sensitivity analysis in mathematical programming," *J. of Optimization Theory and Applications*, vol. 128, no. 1, pp. 49–74, Jan 2006.
[25] E. Castillo, A. J. Conejo, C. Castillo, and R. Mínguez, "Closed formulas in local sensitivity analysis for some classes of linear and non-linear problems," *TOP*, vol. 15, no. 2, pp. 355–371, Dec 2007.
[26] A. J. Conejo, E. Castillo, R. Mínguez, and F. Milano, "Locational marginal price sensitivities," *IEEE Trans. on Power Systems*, vol. 20, no. 4, pp. 2026–2033, Nov 2005.
[27] F. Milano, A. J. Conejo, and R. Zárate-Miñano, "General sensitivity formulas for maximum loading conditions in power systems," *IET Procs on Gen., Transm. and Distr.*, vol. 1, no. 3, pp. 516–526, May 2007.
[28] R. Mínguez and A. J. Conejo, "State estimation sensitivity analysis," *IEEE Trans. on Power Systems*, vol. 22, no. 3, pp. 1080–1091, Aug 2007.
[29] F. Milano, *Power System Modelling and Scripting*. London: Springer, 2010.
[30] A. M. Kettner and M. Paolone, "On the properties of the power systems nodal admittance matrix," *IEEE Trans. on Power Systems*, vol. 33, no. 1, pp. 1130–1131, Jan 2018.
[31] S. Boyd and L. Vandenberghe, *Convex Optimization*. Cambridge, UK: Cambridge University Press, 2004.
[32] P. W. Sauer, M. A. Pai and J. H. Chow, *Power System Dynamics and Stability – With Synchrophasor Measurement and Power System Toolbox*, 2nd ed. New York, US: Wiley-IEEE Press, 2017.
[33] Á. Ortega and F. Milano, "Impact of Frequency Estimation for VSC-based Devices with Primary Frequency Control," in *Procs of the IEEE ISGT Europe*, Turin, Italy, Sep. 2017.
[34] F. Milano, "A Python-based software tool for power system analysis," in *Procs of the IEEE PES General Meeting*, Vancouver, BC, July 2013.
[35] F. Milano and R. Zárate-Miñano, "A systematic method to model power systems as stochastic differential algebraic equations," *IEEE Trans. on Power Systems*, vol. 28, no. 4, pp. 4537–4544, Nov 2013.
[36] J. Qiu, Y. Wei, H. R. Karimi, and H. Gao, "Reliable control of discrete-time piecewise-affine time-delay systems via output feedback," *IEEE Trans. on Reliability*, vol. 67, no. 1, pp. 79–91, March 2018.
[37] A. Nicastri and A. Nagliero, "Comparison and Evaluation of the PLL Techniques for the Design of the Grid-connected Inverter Systems," in *2010 IEEE International Symposium on Industrial Electronics*, July 2010, pp. 3865–3870.

Federico Milano (S'02, M'04, SM'09, F'16) received from the University of Genoa, Italy, the ME and Ph.D. in Electrical Engineering in 1999 and 2003, respectively. From 2001 to 2002 he was with the University of Waterloo, Canada. From 2003 to 2013, he was with the University of Castilla-La Mancha, Spain. In 2013, he joined the University College Dublin, Ireland, where he is currently Professor of Power System Control and Protections and Head of Electrical Engineering. His research interests include power system modeling, operation, stability analysis and control.

Álvaro Ortega (S'14, M'16) received the degree in Industrial Eng. from Escuela Superior de Ingenieros Industriales, Univ. of Castilla-La Mancha, Ciudad Real, Spain, in 2013. In 2017, he received the Ph.D. in Electrical Eng. from Univ. College Dublin, Ireland, where he is currently a senior power systems researcher. His research interests include dynamic modelling and control of energy storage systems, and transient and frequency stability analysis of power systems.

Antonio J. Conejo (F'04) received the M.S. degree from the Massachusetts Institute of Technology, Cambridge, MA, in 1987, and the Ph.D. degree from the Royal Institute of Technology, Stockholm, Sweden, in 1990. He is currently a full professor in the Department of Integrated Systems Engineering and the Department of Electrical and Computer Engineering, The Ohio State University, Columbus, OH. His research interests include control, operations, planning, economics and regulation of electric energy systems, as well as statistics and optimization theory and its applications.

This Article is part of a project that has received funding from the **European Union's Horizon 2020 research and innovation programme under grant agreement Nº727481**